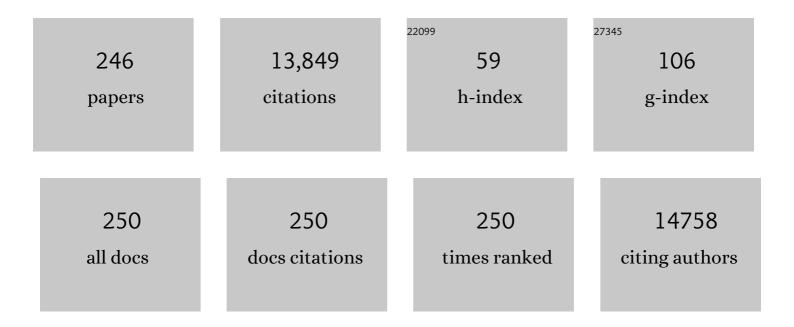
Dai-Wen Pang

List of Publications by Year in descending order

Source: https://exaly.com/author-pdf/468034/publications.pdf Version: 2024-02-01



DAL-WEN DANC

#	Article	IF	CITATIONS
1	Electrochemical Tuning of Luminescent Carbon Nanodots: From Preparation to Luminescence Mechanism. Advanced Materials, 2011, 23, 5801-5806.	11.1	872
2	Facile preparation of low cytotoxicity fluorescent carbon nanocrystals by electrooxidation of graphite. Chemical Communications, 2008, , 5116.	2.2	786
3	Photoluminescenceâ€Tunable Carbon Nanodots: Surfaceâ€State Energyâ€Gap Tuning. Advanced Materials, 2015, 27, 1663-1667.	11.1	658
4	Ultrasmall Near-Infrared Ag ₂ Se Quantum Dots with Tunable Fluorescence for <i>in Vivo</i> Imaging. Journal of the American Chemical Society, 2012, 134, 79-82.	6.6	313
5	Bright quantum dots emitting at â^¼1,600 nm in the NIR-IIb window for deep tissue fluorescence imaging. Proceedings of the National Academy of Sciences of the United States of America, 2018, 115, 6590-6595.	3.3	310
6	Water-soluble Ag2S quantum dots for near-infrared fluorescence imaging inÂvivo. Biomaterials, 2012, 33, 5130-5135.	5.7	288
7	Quick-Response Magnetic Nanospheres for Rapid, Efficient Capture and Sensitive Detection of Circulating Tumor Cells. ACS Nano, 2014, 8, 941-949.	7.3	228
8	Fluorescent-Magnetic-Biotargeting Multifunctional Nanobioprobes for Detecting and Isolating Multiple Types of Tumor Cells. ACS Nano, 2011, 5, 761-770.	7.3	192
9	Ag ₂ Se Quantum Dots with Tunable Emission in the Second Near-Infrared Window. ACS Applied Materials & Interfaces, 2013, 5, 1186-1189.	4.0	188
10	Emission-Tunable Near-Infrared Ag ₂ S Quantum Dots. Chemistry of Materials, 2012, 24, 3-5.	3.2	183
11	Sensitive and Quantitative Detection of C-Reaction Protein Based on Immunofluorescent Nanospheres Coupled with Lateral Flow Test Strip. Analytical Chemistry, 2016, 88, 6577-6584.	3.2	180
12	Living Yeast Cells as a Controllable Biosynthesizer for Fluorescent Quantum Dots. Advanced Functional Materials, 2009, 19, 2359-2364.	7.8	178
13	Shifting and non-shifting fluorescence emitted by carbon nanodots. Journal of Materials Chemistry, 2012, 22, 5917.	6.7	177
14	Molecularly Engineered Macrophageâ€Đerived Exosomes with Inflammation Tropism and Intrinsic Heme Biosynthesis for Atherosclerosis Treatment. Angewandte Chemie - International Edition, 2020, 59, 4068-4074.	7.2	164
15	Near-Infrared Electrogenerated Chemiluminescence of Ultrasmall Ag ₂ Se Quantum Dots for the Detection of Dopamine. Analytical Chemistry, 2012, 84, 8932-8935.	3.2	162
16	Colorimetric-Fluorescent-Magnetic Nanosphere-Based Multimodal Assay Platform for Salmonella Detection. Analytical Chemistry, 2019, 91, 1178-1184.	3.2	152
17	Strongly fluorescent hydrogels with quantum dots embedded in cellulose matrices. Journal of Materials Chemistry, 2009, 19, 7771.	6.7	146
18	Ultrasmall Magnetically Engineered Ag ₂ Se Quantum Dots for Instant Efficient Labeling and Whole-Body High-Resolution Multimodal Real-Time Tracking of Cell-Derived Microvesicles. Journal of the American Chemical Society, 2016, 138, 1893-1903.	6.6	143

#	Article	IF	CITATIONS
19	Cell-Targeting Multifunctional Nanospheres with both Fluorescence and Magnetism. Small, 2005, 1, 506-509.	5.2	142
20	Enzyme-Induced Metallization as a Signal Amplification Strategy for Highly Sensitive Colorimetric Detection of Avian Influenza Virus Particles. Analytical Chemistry, 2014, 86, 2752-2759.	3.2	137
21	Long-term increased grain yield and soil fertility from intercropping. Nature Sustainability, 2021, 4, 943-950.	11.5	137
22	Single-Virus Tracking: From Imaging Methodologies to Virological Applications. Chemical Reviews, 2020, 120, 1936-1979.	23.0	131
23	Magnetic and Folate Functionalization Enables Rapid Isolation and Enhanced Tumor-Targeting of Cell-Derived Microvesicles. ACS Nano, 2017, 11, 277-290.	7.3	130
24	Dual-Signal Readout Nanospheres for Rapid Point-of-Care Detection of Ebola Virus Glycoprotein. Analytical Chemistry, 2017, 89, 13105-13111.	3.2	128
25	Effectively and Efficiently Dissecting the Infection of Influenza Virus by Quantum-Dot-Based Single-Particle Tracking. ACS Nano, 2012, 6, 141-150.	7.3	127
26	One-Step Sensitive Detection of Salmonella typhimurium by Coupling Magnetic Capture and Fluorescence Identification with Functional Nanospheres. Analytical Chemistry, 2013, 85, 1223-1230.	3.2	125
27	Imaging Viral Behavior in Mammalian Cells with Selfâ€Assembled Capsid–Quantumâ€Dot Hybrid Particles. Small, 2009, 5, 718-726.	5.2	120
28	Uniform Fluorescent Nanobioprobes for Pathogen Detection. ACS Nano, 2014, 8, 5116-5124.	7.3	120
29	A Method for the Fabrication of Low-Noise Carbon Fiber Nanoelectrodes. Analytical Chemistry, 2001, 73, 1048-1052.	3.2	114
30	Detection of SARS-CoV-2 by CRISPR/Cas12a-Enhanced Colorimetry. ACS Sensors, 2021, 6, 1086-1093.	4.0	108
31	Tracking single viruses infecting their host cells using quantum dots. Chemical Society Reviews, 2016, 45, 1211-1224.	18.7	106
32	Plasmonic and Photothermal Immunoassay via Enzyme-Triggered Crystal Growth on Gold Nanostars. Analytical Chemistry, 2019, 91, 2086-2092.	3.2	103
33	Mechanism-Oriented Controllability of Intracellular Quantum Dots Formation: The Role of Glutathione Metabolic Pathway. ACS Nano, 2013, 7, 2240-2248.	7.3	96
34	A colorimetric and electrochemical immunosensor for point-of-care detection of enterovirus 71. Biosensors and Bioelectronics, 2018, 99, 186-192.	5.3	94
35	Fluorescent/magnetic micro/nano-spheres based on quantum dots and/or magnetic nanoparticles: preparation, properties, and their applications in cancer studies. Nanoscale, 2016, 8, 12406-12429.	2.8	93
36	Clathrin-Mediated Endocytosis in Living Host Cells Visualized through Quantum Dot Labeling of Infectious Hematopoietic Necrosis Virus. Journal of Virology, 2011, 85, 6252-6262.	1.5	92

#	Article	IF	CITATIONS
37	Intercropping maintains soil fertility in terms of chemical properties and enzyme activities on a timescale of one decade. Plant and Soil, 2015, 391, 265-282.	1.8	89
38	Transformation of Cellâ€Derived Microparticles into Quantumâ€Dotâ€Labeled Nanovectors for Antitumor siRNA Delivery. Angewandte Chemie - International Edition, 2015, 54, 1036-1040.	7.2	86
39	Mechanofluorochromic Carbon Nanodots: Controllable Pressureâ€Triggered Blue―and Redâ€Shifted Photoluminescence. Angewandte Chemie - International Edition, 2018, 57, 1893-1897.	7.2	86
40	Revealing Carbon Nanodots As Coreactants of the Anodic Electrochemiluminescence of Ru(bpy) ₃ ²⁺ . Analytical Chemistry, 2014, 86, 7224-7228.	3.2	83
41	DNA-stabilized silver nanoclusters and carbon nanoparticles oxide: A sensitive platform for label-free fluorescence turn-on detection of HIV-DNA sequences. Biosensors and Bioelectronics, 2016, 85, 837-843.	5.3	82
42	Intercropping Enhances Productivity and Maintains the Most Soil Fertility Properties Relative to Sole Cropping. PLoS ONE, 2014, 9, e113984.	1.1	79
43	Real-Time Monitoring of Nitric Oxide at Single-Cell Level with Porphyrin-Functionalized Graphene Field-Effect Transistor Biosensor. Analytical Chemistry, 2016, 88, 11115-11122.	3.2	78
44	Ultrasmall Pb:Ag ₂ S Quantum Dots with Uniform Particle Size and Bright Tunable Fluorescence in the NIRâ€I Window. Small, 2018, 14, e1703296.	5.2	78
45	Holographic Optical Tweezers and Boosting Upconversion Luminescent Resonance Energy Transfer Combined Clustered Regularly Interspaced Short Palindromic Repeats (CRISPR)/Cas12a Biosensors. ACS Nano, 2021, 15, 8142-8154.	7.3	78
46	A micropillarâ€integrated smart microfluidic device for specific capture and sorting of cells. Electrophoresis, 2007, 28, 4713-4722.	1.3	77
47	A Simple Point-of-Care Microfluidic Immunomagnetic Fluorescence Assay for Pathogens. Analytical Chemistry, 2013, 85, 2645-2651.	3.2	77
48	A chip assisted immunomagnetic separation system for the efficient capture and in situ identification of circulating tumor cells. Lab on A Chip, 2016, 16, 1214-1223.	3.1	75
49	A field effect transistor modified with reduced graphene oxide for immunodetection of Ebola virus. Mikrochimica Acta, 2019, 186, 223.	2.5	74
50	Robust and Highly Sensitive Fluorescence Approach for Point-of-Care Virus Detection Based on Immunomagnetic Separation. Analytical Chemistry, 2012, 84, 2358-2365.	3.2	73
51	An efficient edge-functionalization method to tune the photoluminescence of graphene quantum dots. Nanoscale, 2015, 7, 5969-5973.	2.8	73
52	Reliable Digital Single Molecule Electrochemistry for Ultrasensitive Alkaline Phosphatase Detection. Analytical Chemistry, 2016, 88, 9166-9172.	3.2	73
53	Stable CsPbBr ₃ perovskite quantum dots with high fluorescence quantum yields. New Journal of Chemistry, 2018, 42, 9496-9500.	1.4	71
54	Cell Membraneâ€Camouflaged NIR II Fluorescent Ag ₂ Te Quantum Dotsâ€Based Nanobioprobes for Enhanced In Vivo Homotypic Tumor Imaging. Advanced Healthcare Materials, 2019, 8, e1900341.	3.9	68

#	Article	IF	CITATIONS
55	Digital Single Virus Immunoassay for Ultrasensitive Multiplex Avian Influenza Virus Detection Based on Fluorescent Magnetic Multifunctional Nanospheres. ACS Applied Materials & Interfaces, 2019, 11, 5762-5770.	4.0	66
56	Optically Encoded Multifunctional Nanospheres for One-Pot Separation and Detection of Multiplex DNA Sequences. Analytical Chemistry, 2013, 85, 11929-11935.	3.2	65
57	Breaking through the Size Control Dilemma of Silver Chalcogenide Quantum Dots via Trialkylphosphine-Induced Ripening: Leading to Ag ₂ Te Emitting from 950 to 2100 nm. Journal of the American Chemical Society, 2021, 143, 12867-12877.	6.6	65
58	Fluorescence onverging Carbon Nanodotsâ€Hybridized Silica Nanosphere. Small, 2016, 12, 4702-4706.	5.2	63
59	Wheat Germ Agglutinin-Modified Trifunctional Nanospheres for Cell Recognition. Bioconjugate Chemistry, 2007, 18, 1749-1755.	1.8	62
60	Visualizing the endocytic and exocytic processes of wheat germ agglutinin by quantum dot-based single-particle tracking. Biomaterials, 2011, 32, 7616-7624.	5.7	62
61	Lectin-modified trifunctional nanobiosensors for mapping cell surface glycoconjugates. Biosensors and Bioelectronics, 2009, 24, 1311-1317.	5.3	61
62	High-efficiency dual labeling of influenza virus for single-virus imaging. Biomaterials, 2012, 33, 7828-7833.	5.7	61
63	Real-Time Dissection of Distinct Dynamin-Dependent Endocytic Routes of Influenza A Virus by Quantum Dot-Based Single-Virus Tracking. ACS Nano, 2017, 11, 4395-4406.	7.3	61
64	Nearâ€Infrared Fluorescent Ag ₂ Se–Cetuximab Nanoprobes for Targeted Imaging and Therapy of Cancer. Small, 2017, 13, 1602309.	5.2	61
65	Surface Sensitive Photoluminescence of Carbon Nanodots: Coupling between the Carbonyl Group and ï€-Electron System. Journal of Physical Chemistry Letters, 2019, 10, 3621-3629.	2.1	61
66	Visual Recognition and Efficient Isolation of Apoptotic Cells with Fluorescent-Magnetic-Biotargeting Multifunctional Nanospheres. Clinical Chemistry, 2007, 53, 2177-2185.	1.5	60
67	Electrochemical oxidation of DNA at a gold microelectrode. Electroanalysis, 1995, 7, 774-777.	1.5	59
68	Combination of dynamic magnetophoretic separation and stationary magnetic trap for highly sensitive and selective detection of Salmonella typhimurium in complex matrix. Biosensors and Bioelectronics, 2015, 74, 628-636.	5.3	59
69	A "Driver Switchover―Mechanism of Influenza Virus Transport from Microfilaments to Microtubules. ACS Nano, 2018, 12, 474-484.	7.3	59
70	Ultrasensitive Ebola Virus Detection Based on Electroluminescent Nanospheres and Immunomagnetic Separation. Analytical Chemistry, 2017, 89, 2039-2048.	3.2	58
71	Quantum Dot Based Biotracking and Biodetection. Analytical Chemistry, 2019, 91, 532-547.	3.2	58
72	A multicomponent recognition and separation system established via fluorescent, magnetic, dualencoded multifunctional bioprobes. Biomaterials, 2011, 32, 1177-1184.	5.7	57

#	Article	IF	CITATIONS
73	A boosting upconversion luminescent resonance energy transfer and biomimetic periodic chip integrated CRISPR/Cas12a biosensor for functional DNA regulated transduction of non-nucleic acid targets. Biosensors and Bioelectronics, 2020, 169, 112650.	5.3	57
74	Photoinduced Electron Transfer Mediated by Coordination between Carboxyl on Carbon Nanodots and Cu ²⁺ Quenching Photoluminescence. Journal of Physical Chemistry C, 2018, 122, 3662-3668.	1.5	56
75	The quantitative detection of total HER2 load by quantum dots and the identification of a new subtype of breast cancer with different 5-year prognosis. Biomaterials, 2010, 31, 8818-8825.	5.7	55
76	Bifunctional magnetic nanobeads for sensitive detection of avian influenza A (H7N9) virus based on immunomagnetic separation and enzyme-induced metallization. Biosensors and Bioelectronics, 2015, 68, 586-592.	5.3	54
77	Digital Single Virus Electrochemical Enzyme-Linked Immunoassay for Ultrasensitive H7N9 Avian Influenza Virus Counting. Analytical Chemistry, 2018, 90, 1683-1690.	3.2	53
78	A virus-induced kidney disease model based on organ-on-a-chip: Pathogenesis exploration of virus-related renal dysfunctions. Biomaterials, 2019, 219, 119367.	5.7	53
79	Ebola Virus Aptamers: From Highly Efficient Selection to Application on Magnetism-Controlled Chips. Analytical Chemistry, 2019, 91, 3367-3373.	3.2	53
80	Myosin-Driven Intercellular Transportation of Wheat Germ Agglutinin Mediated by Membrane Nanotubes between Human Lung Cancer Cells. ACS Nano, 2012, 6, 10033-10041.	7.3	52
81	Nanosphere-based one-step strategy for efficient and nondestructive detection of circulating tumor cells. Biosensors and Bioelectronics, 2017, 94, 219-226.	5.3	52
82	Globally Visualizing the Microtubule-Dependent Transport Behaviors of Influenza Virus in Live Cells. Analytical Chemistry, 2014, 86, 3902-3908.	3.2	51
83	Chip-Assisted Single-Cell Biomarker Profiling of Heterogeneous Circulating Tumor Cells Using Multifunctional Nanospheres. Analytical Chemistry, 2018, 90, 10518-10526.	3.2	50
84	One-to-Many Single Entity Electrochemistry Biosensing for Ultrasensitive Detection of microRNA. Analytical Chemistry, 2020, 92, 853-858.	3.2	50
85	Photocatalysis-Induced Renewable Field-Effect Transistor for Protein Detection. Analytical Chemistry, 2016, 88, 4048-4054.	3.2	49
86	Efficient Enrichment and Analyses of Bacteria at Ultralow Concentration with Quick-Response Magnetic Nanospheres. ACS Applied Materials & Interfaces, 2017, 9, 9416-9425.	4.0	49
87	Pathological hydrogen peroxide triggers the fibrillization of wild-type SOD1 via sulfenic acid modification of Cys-111. Cell Death and Disease, 2018, 9, 67.	2.7	49
88	Labeling the nucleocapsid of enveloped baculovirus with quantum dots for single-virus tracking. Biomaterials, 2014, 35, 2295-2301.	5.7	48
89	Folate-Engineered Microvesicles for Enhanced Target and Synergistic Therapy toward Breast Cancer. ACS Applied Materials & Interfaces, 2017, 9, 5100-5108.	4.0	48
90	Multifunctional Screening Platform for the Highly Efficient Discovery of Aptamers with High Affinity and Specificity. Analytical Chemistry, 2017, 89, 6535-6542.	3.2	47

#	Article	IF	CITATIONS
91	Fast and High-Accuracy Localization for Three-Dimensional Single-Particle Tracking. Scientific Reports, 2013, 3, 2462.	1.6	46
92	Ultrasensitive Electrochemiluminescence Biosensor Based on Closed Bipolar Electrode for Alkaline Phosphatase Detection in Single Liver Cancer Cell. Analytical Chemistry, 2021, 93, 1757-1763.	3.2	46
93	Energy-Level-Related Response of Cathodic Electrogenerated-Chemiluminescence of Self-Assembled CdSe/ZnS Quantum Dot Films. Journal of Physical Chemistry C, 2011, 115, 18822-18828.	1.5	45
94	Quantum-dots based simultaneous detection of multiple biomarkers of tumor stromal features to predict clinical outcomes in gastric cancer. Biomaterials, 2012, 33, 5742-5752.	5.7	45
95	Rapid detection and subtyping of multiple influenza viruses on a microfluidic chip integrated with controllable micro-magnetic field. Biosensors and Bioelectronics, 2018, 100, 348-354.	5.3	45
96	Gd-DTPA-coupled Ag ₂ Se quantum dots for dual-modality magnetic resonance imaging and fluorescence imaging in the second near-infrared window. Nanoscale, 2018, 10, 10699-10704.	2.8	45
97	Ultrasensitive electrochemical detection of microRNA-21 with wide linear dynamic range based on dual signal amplification. Biosensors and Bioelectronics, 2019, 131, 267-273.	5.3	45
98	Indirect immunofluorescence detection of E. coli O157:H7 with fluorescent silica nanoparticles. Biosensors and Bioelectronics, 2015, 66, 95-102.	5.3	44
99	Electrochemical Methods to Study Photoluminescent Carbon Nanodots: Preparation, Photoluminescence Mechanism and Sensing. ACS Applied Materials & Interfaces, 2016, 8, 28372-28382.	4.0	44
100	Quantum Dots: A Promising Fluorescent Label for Probing Virus Trafficking. Accounts of Chemical Research, 2021, 54, 2991-3002.	7.6	44
101	Nearâ€Infraredâ€II Quantum Dots for In Vivo Imaging and Cancer Therapy. Small, 2022, 18, e2104567.	5.2	44
102	Simultaneous Point-of-Care Detection of Enterovirus 71 and Coxsackievirus B3. Analytical Chemistry, 2015, 87, 11105-11112.	3.2	43
103	Surface Labeling of Enveloped Viruses Assisted by Host Cells. ACS Chemical Biology, 2012, 7, 683-688.	1.6	42
104	Self-biotinylation and site-specific double labeling of baculovirus using quantum dots for single-virus in-situ tracking. Biomaterials, 2013, 34, 7506-7518.	5.7	42
105	Clicking Hydrazine and Aldehyde: The Way to Labeling of Viruses with Quantum Dots. ACS Nano, 2015, 9, 11750-11760.	7.3	42
106	MnCaCs-Biomineralized Oncolytic Virus for Bimodal Imaging-Guided and Synergistically Enhanced Anticancer Therapy. Nano Letters, 2019, 19, 8002-8009.	4.5	41
107	Controlling the Magnetic Field Distribution on the Micrometer Scale and Generation of Magnetic Bead Patterns for Microfluidic Applications. Langmuir, 2011, 27, 5147-5156.	1.6	40
108	Fluorescent–magnetic dual-encoded nanospheres: a promising tool for fast-simultaneous-addressable high-throughput analysis. Nanotechnology, 2012, 23, 035602.	1.3	40

#	Article	IF	CITATIONS
109	Near-infrared Ag ₂ Se quantum dots with distinct absorption features and high fluorescence quantum yields. RSC Advances, 2016, 6, 38183-38186.	1.7	40
110	Labeling viral envelope lipids with quantum dots by harnessing the biotinylated lipid-self-inserted cellular membrane. Biomaterials, 2016, 106, 69-77.	5.7	40
111	Threeâ€Dimensional Tracking of Rab5―and Rab7â€Associated Infection Process of Influenza Virus. Small, 2014, 10, 4746-4753.	5.2	37
112	Biofunctionalized magnetic nanospheres-based cell sorting strategy for efficient isolation, detection and subtype analyses of heterogeneous circulating hepatocellular carcinoma cells. Biosensors and Bioelectronics, 2016, 85, 633-640.	5.3	36
113	Spectrally Combined Encoding for Profiling Heterogeneous Circulating Tumor Cells Using a Multifunctional Nanosphereâ€Mediated Microfluidic Platform. Angewandte Chemie - International Edition, 2020, 59, 11240-11244.	7.2	36
114	Quantum Dots-Based Quantitative and In Situ Multiple Imaging on Ki67 and Cytokeratin to Improve Ki67 Assessment in Breast Cancer. PLoS ONE, 2015, 10, e0122734.	1.1	36
115	Multipole-plasmon-enhanced förster energy transfer between semiconductor quantum dots via dual-resonance nanoantenna effects. Applied Physics Letters, 2010, 96, 043106.	1.5	35
116	Clickable Gold Nanoparticles as the Building Block of Nanobioprobes. Langmuir, 2010, 26, 10171-10176.	1.6	34
117	Controllable synthesis of PbSe nanocubes in aqueous phase using a quasi-biosystem. Journal of Materials Chemistry, 2012, 22, 3713.	6.7	34
118	Cytotoxicity of nucleus-targeting fluorescent gold nanoclusters. Nanoscale, 2014, 6, 13126-13134.	2.8	34
119	Dual Amplification Fluorescence Assay for Alpha Fetal Protein Utilizing Immunohybridization Chain Reaction and Metal-Enhanced Fluorescence of Carbon Nanodots. ACS Applied Materials & Interfaces, 2017, 9, 37606-37614.	4.0	34
120	Assembly-enhanced fluorescence from metal nanoclusters and quantum dots for highly sensitive biosensing. Sensors and Actuators B: Chemical, 2019, 279, 334-341.	4.0	33
121	Synthesis of sub-5 nm Au–Ag alloy nanoparticles using bio-reducing agent in aqueous solution. Journal of Materials Chemistry, 2011, 21, 17080.	6.7	32
122	One-to-one quantum dot-labeled single long DNA probes. Biomaterials, 2011, 32, 5471-5477.	5.7	32
123	Rapid and Quantitative Detection of Avian Influenza A(H7N9) Virions in Complex Matrices Based on Combined Magnetic Capture and Quantum Dot Labeling. Small, 2015, 11, 5280-5288.	5.2	32
124	Singleâ€Particle Tracking Reveals the Sequential Entry Process of the Bunyavirus Severe Fever with Thrombocytopenia Syndrome Virus. Small, 2019, 15, e1803788.	5.2	31
125	Electrochemical Monitoring of Hydrogen Sulfide Release from Single Cells. ChemElectroChem, 2016, 3, 1998-2002.	1.7	30
126	Simultaneous Visualization of Parental and Progeny Viruses by a Capsid-Specific HaloTag Labeling Strategy. ACS Nano, 2016, 10, 1147-1155.	7.3	30

#	Article	IF	CITATIONS
127	Combining Holographic Optical Tweezers with Upconversion Luminescence Encoding: Imaging-Based Stable Suspension Array for Sensitive Responding of Dual Cancer Biomarkers. Analytical Chemistry, 2018, 90, 2639-2647.	3.2	30
128	Glucose-functionalized near-infrared Ag ₂ Se quantum dots with renal excretion ability for long-term <i>in vivo</i> tumor imaging. Journal of Materials Chemistry B, 2019, 7, 5782-5788.	2.9	30
129	Droplet-based microreactor for synthesis of water-soluble Ag ₂ S quantum dots. Nanotechnology, 2015, 26, 275701.	1.3	28
130	Metal-enhanced fluorescence of gold nanoclusters as a sensing platform for multi-component detection. Sensors and Actuators B: Chemical, 2019, 282, 650-658.	4.0	28
131	Phase Separation and Cytotoxicity of Tau are Modulated by Protein Disulfide Isomerase and S-nitrosylation of this Molecular Chaperone. Journal of Molecular Biology, 2020, 432, 2141-2163.	2.0	28
132	Dissecting the Factors Affecting the Fluorescence Stability of Quantum Dots in Live Cells. ACS Applied Materials & Interfaces, 2016, 8, 8401-8408.	4.0	27
133	Effect of POE-g-GMA on mechanical, rheological and thermal properties of poly(lactic) Tj ETQq1 1 0.784314 rgBT	/Qverlock 1.7	10 Tf 50 5(
134	Quantitatively Switchable pH-Sensitive Photoluminescence of Carbon Nanodots. Journal of Physical Chemistry Letters, 2021, 12, 2727-2735.	2.1	27
135	One-Step Monitoring of Multiple Enterovirus 71 Infection-Related MicroRNAs Using Core–Satellite Structure of Magnetic Nanobeads and Multicolor Quantum Dots. Analytical Chemistry, 2020, 92, 830-837.	3.2	26
136	Quantum dot-based quantitative immunofluorescence detection and spectrum analysis of epidermal growth factor receptor in breast cancer tissue arrays. International Journal of Nanomedicine, 2011, 6, 2265.	3.3	25
137	Exploring Sialic Acid Receptorsâ€Related Infection Behavior of Avian Influenza Virus in Human Bronchial Epithelial Cells by Singleâ€Particle Tracking. Small, 2014, 10, 2712-2720.	5.2	24
138	Biometallizationâ€Based Electrochemical Magnetoimmunosensing Strategy for Avian Influenza A (H7N9) Virus Particle Detection. Chemistry - an Asian Journal, 2015, 10, 1387-1393.	1.7	24
139	Lipid-Specific Labeling of Enveloped Viruses with Quantum Dots for Single-Virus Tracking. MBio, 2020, 11, .	1.8	24
140	Ag ₂ Te Quantum Dots as Contrast Agents for Near-Infrared Fluorescence and Computed Tomography Imaging. ACS Applied Nano Materials, 2020, 3, 6071-6077.	2.4	24
141	Fluorescence Detection of H5N1 Virus Gene Sequences Based on Optical Tweezers with Two-Photon Excitation Using a Single Near Infrared Nanosecond Pulse Laser. Analytical Chemistry, 2016, 88, 4432-4439.	3.2	23
142	Transformation of Viral Light Particles into Near-Infrared Fluorescence Quantum Dot-Labeled Active Tumor-Targeting Nanovectors for Drug Delivery. Nano Letters, 2019, 19, 7035-7042.	4.5	23
143	Kineticsâ€Controlled Formation of Gold Clusters Using a Quasiâ€Biological System. Advanced Functional Materials, 2010, 20, 3673-3677.	7.8	22
144	Control of magnetic field distribution by using nickel powder@PDMS pillars in microchannels. RSC Advances, 2014, 4, 17660-17666.	1.7	22

#	Article	IF	CITATIONS
145	A fluorescent aptasensor using double-stranded DNA/graphene oxide as the indicator probe. Biosensors and Bioelectronics, 2016, 78, 431-437.	5.3	22
146	Uncovering the Rab5â€Independent Autophagic Trafficking of Influenza A Virus by Quantumâ€Dotâ€Based Singleâ€Virus Tracking. Small, 2018, 14, e1702841.	5.2	22
147	Cellular-Beacon-Mediated Counting for the Ultrasensitive Detection of Ebola Virus on an Integrated Micromagnetic Platform. Analytical Chemistry, 2018, 90, 7310-7317.	3.2	22
148	Visualization of Vaccine Dynamics with Quantum Dots for Immunotherapy. Angewandte Chemie - International Edition, 2021, 60, 24275-24283.	7.2	22
149	Magnetic Chip Based Extracorporeal Circulation: A New Tool for Circulating Tumor Cell in Vivo Detection. Analytical Chemistry, 2019, 91, 15260-15266.	3.2	21
150	Breaking Through Bead-Supported Assay: Integration of Optical Tweezers Assisted Fluorescence Imaging and Luminescence Confined Upconversion Nanoparticles Triggered Luminescent Resonance Energy Transfer (LRET). Analytical Chemistry, 2019, 91, 7950-7957.	3.2	21
151	Precision photothermal therapy and photoacoustic imaging by <i>in situ</i> activatable thermoplasmonics. Chemical Science, 2021, 12, 10097-10105.	3.7	21
152	Intermediate-dominated controllable biomimetic synthesis of gold nanoparticles in a quasi-biological system. Nanoscale, 2010, 2, 2120.	2.8	20
153	Harnessing Intracellular Biochemical Pathways for In Vitro Synthesis of Designer Tellurium Nanorods. Small, 2015, 11, 5416-5422.	5.2	19
154	Target-triggered signal turn-on detection of prostate specific antigen based on metal-enhanced fluorescence of Ag@SiO ₂ @SiO ₂ -RuBpy composite nanoparticles. Nanotechnology, 2017, 28, 065501.	1.3	19
155	Integrating optical tweezers with up-converting luminescence: a non-amplification analytical platform for quantitative detection of microRNA-21 sequences. Chemical Communications, 2017, 53, 4092-4095.	2.2	19
156	Neutralizing Mutations Significantly Inhibit Amyloid Formation by Human Prion Protein and Decrease Its Cytotoxicity. Journal of Molecular Biology, 2020, 432, 828-844.	2.0	19
157	CdZnSeS quantum dots condensed with ordered mesoporous carbon for high-sensitive electrochemiluminescence detection of hydrogen peroxide in live cells. Electrochimica Acta, 2020, 362, 137107.	2.6	19
158	PEC-interspersed nitrilotriacetic acid-functionalized quantum dots for site-specific labeling of prion proteins expressed on cell surfaces. Biomaterials, 2010, 31, 8362-8370.	5.7	18
159	Sensitive multiplexed DNA detection using silica nanoparticles as the target capturing platform. Talanta, 2014, 128, 263-267.	2.9	18
160	Revealing the biodistribution and clearance of Ag ₂ Se near-infrared quantum dots in mice. New Journal of Chemistry, 2017, 41, 12721-12725.	1.4	18
161	A High Throughput Micro-Chamber Array Device for Single Cell Clonal Cultivation and Tumor Heterogeneity Analysis. Scientific Reports, 2015, 5, 11937.	1.6	17
162	Intracellular self-assembly based multi-labeling of key viral components: Envelope, capsid and nucleic acids. Biomaterials, 2016, 99, 24-33.	5.7	17

#	Article	IF	CITATIONS
163	Preparation of Monodisperse Hydrophilic Quantum Dots with Amphiphilic Polymers. ACS Applied Materials & Interfaces, 2017, 9, 39901-39906.	4.0	17
164	One-step separation-free detection of carcinoembryonic antigen in whole serum: Combination of two-photon excitation fluorescence and optical trapping. Biosensors and Bioelectronics, 2017, 90, 146-152.	5.3	17
165	Real-Time Monitoring of Temperature Variations around a Gold Nanobipyramid Targeted Cancer Cell under Photothermal Heating by Actively Manipulating an Optically Trapped Luminescent Upconversion Microparticle. Analytical Chemistry, 2020, 92, 1292-1300.	3.2	17
166	Integrating 808 nm Light-Excited Upconversion Luminescence Powering with DNA Tetrahedron Protection: An Exceptionally Precise and Stable Nanomachine for Intracelluar MicroRNA Tracing. ACS Sensors, 2020, 5, 199-207.	4.0	17
167	A room-temperature method for coating a ZnS shell on semiconductor quantum dots. Journal of Materials Chemistry C, 2015, 3, 964-967.	2.7	16
168	A highly reactive chalcogenide precursor for the synthesis of metal chalcogenide quantum dots. Nanoscale, 2015, 7, 19310-19316.	2.8	16
169	Colorimetric and visual determination of DNase I activity using gold nanoparticles as an indicator. Mikrochimica Acta, 2017, 184, 101-106.	2.5	16
170	Multifunctional Cellular Beacons with in Situ Synthesized Quantum Dots Make Pathogen Detectable with the Naked Eye. Analytical Chemistry, 2019, 91, 7280-7287.	3.2	16
171	Ultrasmall Quantum Dots with Broadâ€5pectrum Metal Doping Ability for Trimodal Molecular Imaging. Advanced Functional Materials, 2019, 29, 1901671.	7.8	16
172	Simple and rapid extracellular vesicles quantification via membrane biotinylation strategy coupled with fluorescent nanospheres-based lateral flow assay. Talanta, 2019, 200, 408-414.	2.9	16
173	Development of a Dualâ€Modally Traceable Nanoplatform for Cancer Theranostics Using Natural Circulating Cellâ€Đerived Microparticles in Oral Cancer Patients. Advanced Functional Materials, 2017, 27, 1703482.	7.8	16
174	Determination of the Absolute Number Concentration of Nanoparticles and the Active Affinity Sites on Their Surfaces. Analytical Chemistry, 2016, 88, 10134-10142.	3.2	15
175	Microvesicle detection by a reduced graphene oxide field-effect transistor biosensor based on a membrane biotinylation strategy. Analyst, The, 2019, 144, 6055-6063.	1.7	15
176	Controlled Release of Therapeutic Agents with Near-Infrared Laser for Synergistic Photochemotherapy toward Cervical Cancer. Analytical Chemistry, 2019, 91, 6555-6560.	3.2	15
177	A liquid biopsy-guided drug release system for cancer theranostics: integrating rapid circulating tumor cell detection and precision tumor therapy. Lab on A Chip, 2020, 20, 1418-1425.	3.1	15
178	Visual and efficient immunosensor technique for advancing biomedical applications of quantum dots on Salmonella detection and isolation. Nanoscale, 2016, 8, 4688-4698.	2.8	14
179	Coating Magnetic Nanospheres with PEG To Reduce Nonspecific Adsorption on Cells. ACS Omega, 2019, 4, 7391-7399.	1.6	14
180	Evaluation of Luminescence Properties of Single Hydrophilic Upconversion Nanoparticles by Optical Trapping. Journal of Physical Chemistry C, 2019, 123, 10107-10113.	1.5	14

#	Article	IF	CITATIONS
181	Molecularly Engineered Macrophageâ€Derived Exosomes with Inflammation Tropism and Intrinsic Heme Biosynthesis for Atherosclerosis Treatment. Angewandte Chemie, 2020, 132, 4097-4103.	1.6	14
182	Dual-component gene detection for H7N9 virus – The combination of optical trapping and bead-based fluorescence assay. Biosensors and Bioelectronics, 2016, 86, 1031-1037.	5.3	13
183	Purification of quantum dot-based bioprobes via high-performance size exclusion chromatography. Talanta, 2016, 159, 64-73.	2.9	13
184	Real-Time Dissecting the Entry and Intracellular Dynamics of Single Reovirus Particle. Frontiers in Microbiology, 2018, 9, 2797.	1.5	13
185	Equipping Inner Central Components of Influenza A Virus with Quantum Dots. Analytical Chemistry, 2018, 90, 14020-14028.	3.2	13
186	Internalization of the pseudorabies virus <i>via</i> macropinocytosis analyzed by quantum dot-based single-virus tracking. Chemical Communications, 2018, 54, 11184-11187.	2.2	13
187	Chemoenzymatic Labeling of Extracellular Vesicles for Visualizing Their Cellular Internalization in Real Time. Analytical Chemistry, 2020, 92, 2103-2111.	3.2	13
188	Accurate and Efficient Lipoprotein Detection Based on the HCR–DNAzyme Platform. Analytical Chemistry, 2021, 93, 6128-6134.	3.2	13
189	DNA-Modified Electrodes. Part 5. Electrochemical Behavior of Co2+ at DNA-Modified Gold Electrodes in the Presence of 2,2'-Bipyridyl Analytical Sciences, 1999, 15, 471-475.	0.8	12
190	Powder Microelectrodes for Capillary Electrophoresis with Amperometric Detection Analytical Sciences, 2000, 16, 807-810.	0.8	12
191	Anisotropic cell-to-cell spread of vaccinia virus on microgrooved substrate. Biomaterials, 2014, 35, 5049-5055.	5.7	12
192	Sequence-dependent abnormal aggregation of human Tau fragment in an inducible cell model. Biochimica Et Biophysica Acta - Molecular Basis of Disease, 2015, 1852, 1561-1573.	1.8	12
193	Improving Flow Bead Assay: Combination of Near-Infrared Optical Tweezers Stabilizing and Upconversion Luminescence Encoding. Analytical Chemistry, 2020, 92, 5258-5266.	3.2	12
194	Biomimetic Chip Enhanced Time-Gated Luminescent CRISPR-Cas12a Biosensors under Functional DNA Regulation. Analytical Chemistry, 2021, 93, 12514-12523.	3.2	12
195	Incorporating luminescence-concentrating upconversion nanoparticles and DNA walkers into optical tweezers assisted imaging: a highly stable and ultrasensitive bead supported assay. Chemical Communications, 2020, 56, 6997-7000.	2.2	12
196	Recognition Kinetics of Biomolecules at the Surface of Different-Sized Spheres. Biophysical Journal, 2014, 107, 165-173.	0.2	11
197	Evaluation of nonspecific interactions between quantum dots and proteins. Physical Chemistry Chemical Physics, 2014, 16, 7677.	1.3	11
198	Knockdown of Y-box-binding protein-1 inhibits the malignant progression of HT-29 colorectal adenocarcinoma cells by reversing epithelial-mesenchymal transition. Molecular Medicine Reports, 2014, 10, 2720-2728.	1.1	11

#	Article	IF	CITATIONS
199	Tracking single baculovirus retrograde transportation in host cell via quantum dot-labeling of virus internal component. Journal of Nanobiotechnology, 2017, 15, 37.	4.2	11
200	Real-Time Dissecting the Dynamics of Drug Transportation in the Live Brain. Nano Letters, 2021, 21, 642-650.	4.5	11
201	Water-Soluble High-Quality Ag ₂ Te Quantum Dots Prepared by Mutual Adaptation of Synthesis and Surface Modification for In Vivo Imaging. ACS Applied Bio Materials, 2021, 4, 7692-7700.	2.3	11
202	An exonuclease III-aided "turn-on―fluorescence assay for mercury ions based on graphene oxide and metal-mediated "molecular beacon― RSC Advances, 2015, 5, 12994-12999.	1.7	10
203	Interfacial Synthesis of Ag 2 S/ZnS Core/Shell Quantum Dots in a Droplet Microreactor. ChemistrySelect, 2020, 5, 5889-5894.	0.7	10
204	Designer cell-self-implemented labeling of microvesicles in situ with the intracellular-synthesized quantum dots. Science China Chemistry, 2020, 63, 448-453.	4.2	10
205	Influenza A Viruses Enter Host Cells via Extracellular Ca ²⁺ Influx-Involved Clathrin-Mediated Endocytosis. ACS Applied Bio Materials, 2021, 4, 2044-2051.	2.3	10
206	Artificially regulated synthesis of nanocrystals in live cells. National Science Review, 2022, 9, .	4.6	10
207	Regulation of Silver Precursor Reactivity via Tertiary Phosphine to Synthesize Near-Infrared Ag ₂ Te with Photoluminescence Quantum Yield of up to 14.7%. Chemistry of Materials, 2021, 33, 9524-9533.	3.2	10
208	Immunoprofiling of Severity and Stage of Bacterial Infectious Diseases by Ultrabright Fluorescent Nanosphere-Based Dyad Test Strips. Analytical Chemistry, 2022, 94, 8818-8826.	3.2	10
209	Enhanced and High-Purity Enrichment of Circulating Tumor Cells Based on Immunomagnetic Nanospheres. ACS Applied Nano Materials, 2018, 1, 4019-4027.	2.4	9
210	Ultrasmall MnSe Nanoparticles as <i>T</i> ₁ -MRI Contrast Agents for <i>In Vivo</i> Tumor Imaging. ACS Applied Materials & Interfaces, 2022, 14, 11167-11176.	4.0	9
211	Quantum Dots Tracking Endocytosis and Transport of Proteins Displayed by Mammalian Cells. Analytical Chemistry, 2022, 94, 7567-7575.	3.2	9
212	Generation of sub-femtoliter droplet by T-junction splitting on microfluidic chips. Applied Physics Letters, 2013, 102, 123502.	1.5	8
213	Dynamic monitoring of membrane nanotubes formation induced by vaccinia virus on a high throughput microfluidic chip. Scientific Reports, 2017, 7, 44835.	1.6	8
214	Diffusion Behaviors of Water-Soluble CdSe/ZnS Core/Shell Quantum Dots Investigated by Single-Particle Tracking. Journal of Physical Chemistry C, 2008, 112, 18904-18910.	1.5	7
215	Surface chemistry tuning the selectivity of carbon nanodots towards Hg2+ recognition. Analytica Chimica Acta, 2021, 1146, 33-40.	2.6	7
216	Size-Resolved Single Entity Collision Biosensing for Dual Quantification of MicroRNAs in a Single Run. ACS Applied Materials & Interfaces, 2021, 13, 22254-22261.	4.0	7

#	Article	IF	CITATIONS
217	In-situ quantitation of genome release of Japanese encephalitis viruses by quantum dot-based single-virus tracking. Nano Today, 2021, 40, 101271.	6.2	7
218	Precise selection of aptamers targeting PD-L1 positive small extracellular vesicles on magnetic chips. Chemical Communications, 2021, 57, 3555-3558.	2.2	7
219	Site-specific labeling of baculovirus in an integrated microfluidic device. Lab on A Chip, 2013, 13, 860.	3.1	6
220	Economical synthesis of ultra-small Bi ₂ S ₃ nanoparticles for high-sensitive CT imaging. Materials Research Express, 2019, 6, 095005.	0.8	6
221	Sphingomyelin-Sequestered Cholesterol Domain Recruits Formin-Binding Protein 17 for Constricting Clathrin-Coated Pits in Influenza Virus Entry. Journal of Virology, 2022, 96, JVI0181321.	1.5	6
222	Preparation of RuBpy-doped Silica Fluorescent Nanoprobes and Their Applications to the Recognition of Liver Cancer Cells. Chinese Journal of Analytical Chemistry, 2014, 42, 326-331.	0.9	5
223	Using optical tweezers to construct an upconversion luminescent resonance energy transfer analytical platform. Sensors and Actuators B: Chemical, 2019, 282, 790-797.	4.0	5
224	A near-infrared-II fluorescence anisotropy strategy for separation-free detection of adenosine triphosphate in complex media. Talanta, 2021, 223, 121721.	2.9	5
225	Spatiotemporal Quantification of Endosomal Acidification on the Viral Journey. Small, 2022, 18, e2104200.	5.2	5
226	How different are the surfaces of semiconductor Ag2Se quantum dots with various sizes?. Science Bulletin, 2022, 67, 619-625.	4.3	5
227	Synthesis, magnetic properties, DNA binding and cleavage activity of a new oxalato bridged copper(II) complex. Applied Organometallic Chemistry, 2012, 26, 511-517.	1.7	4
228	Mechanofluorochromic Carbon Nanodots: Controllable Pressureâ€Triggered Blue―and Redâ€Shifted Photoluminescence. Angewandte Chemie, 2018, 130, 1911-1915.	1.6	4
229	Spectrally Combined Encoding for Profiling Heterogeneous Circulating Tumor Cells Using a Multifunctional Nanosphereâ€Mediated Microfluidic Platform. Angewandte Chemie, 2020, 132, 11336-11340.	1.6	4
230	Revealing Microtubule-Dependent Slow-Directed Motility by Single-Particle Tracking. Analytical Chemistry, 2021, 93, 5211-5217.	3.2	4
231	Proximity-induced exponential amplification reaction triggered by proteins and small molecules. Chemical Communications, 2021, 57, 4714-4717.	2.2	4
232	Uncovering the F-Actin-Based Nuclear Egress Mechanism of Newly Synthesized Influenza A Virus Ribonucleoprotein Complexes by Single-Particle Tracking. Analytical Chemistry, 2022, 94, 5624-5633.	3.2	4
233	Optical tweezers assisted analyzing and sorting of tumor cells tagged with fluorescence nanospheres in a microfluidic chip. Sensors and Actuators B: Chemical, 2022, 368, 132173.	4.0	4
234	Chlorophyll-Based Near-Infrared Fluorescent Nanocomposites: Preparation and Optical Properties. ACS Omega, 2020, 5, 14261-14266.	1.6	3

#	Article	IF	CITATIONS
235	Visualization of Vaccine Dynamics with Quantum Dots for Immunotherapy. Angewandte Chemie, 2021, 133, 24477-24485.	1.6	3
236	Quantum Dots with a Compact Amphiphilic Zwitterionic Coating. ACS Applied Materials & Interfaces, 2022, 14, 28097-28104.	4.0	3
237	A method for the statistical evaluation of the fluorescence intensity of single blinking quantum dots using a confocal fluorescence microscope. Analyst, The, 2020, 145, 3131-3135.	1.7	2
238	Current status and future trends of vaccine development against viral infection and disease. New Journal of Chemistry, 2021, 45, 7437-7449.	1.4	2
239	Cancer Treatment: Development of a Dualâ€Modally Traceable Nanoplatform for Cancer Theranostics Using Natural Circulating Cellâ€Đerived Microparticles in Oral Cancer Patients (Adv. Funct. Mater.) Tj ETQq1 1 0.	.78 748 14 rg	gBT /Overloc
240	Nanoscale & Nanoscale Advances joint themed collection on nanocarbons. Nanoscale, 2019, 11, 14097-14098.	2.8	1
241	Bunyaviruses: Singleâ€Particle Tracking Reveals the Sequential Entry Process of the Bunyavirus Severe Fever with Thrombocytopenia Syndrome Virus (Small 6/2019). Small, 2019, 15, 1970032.	5.2	1
242	A salt-out strategy for purification of amphiphilic polymer-coated quantum dots. New Journal of Chemistry, 2020, 44, 15341-15344.	1.4	1
243	Host-cell-assisted construction of a folate-engineered nanocarrier based on viral light particles for targeted cancer therapy. Nanoscale, 2021, 13, 17881-17889.	2.8	1
244	Quantum Dot-Based Dual-Color In Situ Fluorescence Imaging of the Coevolution of CD68 and CD47 in Breast Cancer. ACS Applied Nano Materials, 2022, 5, 1200-1208.	2.4	1
245	Virus imaging: Small 6/2009. Small, 2009, 5, NA-NA.	5.2	0
246	Absolute quantification of particle number concentration using a digital single particle counting system. Mikrochimica Acta, 2019, 186, 529.	2.5	0